

## Article

# Design, Development, and Testing of a Low-Cost Sub-Joule $\mu$ PPT for a Pocket-Cube

Farouk Smith \*  and Jieun Bae

Department of Mechatronics, Nelson Mandela University, Port Elizabeth 6031, South Africa

\* Correspondence: farouk.smith@mandela.ac.za

**Abstract:** This paper presents the design and development of a sub-joule micro-Pulsed Plasma Thruster ( $\mu$ PPT) as a possible low-cost propulsion solution for Pocket-Cubes, used to increase its reliability, capability, and lifetime. It is shown that the  $\mu$ PPT successfully met Pocket-Cube design standards and additional requirements using the iterative design method, focused mainly on simplification and improvements to a traditional PPT design, the utilization of commercial-off-the-shelf (COTS) components and 3D printing. The  $\mu$ PPT was designed to operate and be controlled from an Arduino UNO with a main bank energy of 0.118 J to 0.272 J and power consumption of 0.5 W. It was successfully tested for performance and lifetime in a vacuum chamber ( $-720$  mmHg to  $-96$  kPa) with the use of a micro-pendulum test stand and a high-speed camera. The thruster was tested for its designed operation parameters of 3.3 V and 5 V at a pulsed frequency of 0.25/0.5 Hz. The test results showed that the optimal performance of the thruster with an input voltage supply of 5 V at a pulse frequency of 0.5 Hz, achieved a minimal impulse bit of 0.698  $\mu$ Ns and thrust range of 0.349–1.071  $\mu$ N. A comparison to the STRaND-1 3U CubeSat's PPT performance data showed that the developed  $\mu$ PPT is a competitive propulsion solution, as it achieved more thrust with a similar minimal impulse bit, using only one-third of the power consumption. During the lifetime testing, the  $\mu$ PPT was able to produce 1980 shots.

**Keywords:** microsatellites; pocket-cubes; pulsed plasma thruster; space vehicle propulsion



**Citation:** Smith, F.; Bae, J. Design, Development, and Testing of a Low-Cost Sub-Joule  $\mu$ PPT for a Pocket-Cube. *Aerospace* **2023**, *10*, 316. <https://doi.org/10.3390/aerospace10030316>

Academic Editor: Angelo Cervone

Received: 3 February 2023

Revised: 19 March 2023

Accepted: 20 March 2023

Published: 22 March 2023



**Copyright:** © 2023 by the authors. Licensee MDPI, Basel, Switzerland. This article is an open access article distributed under the terms and conditions of the Creative Commons Attribution (CC BY) license (<https://creativecommons.org/licenses/by/4.0/>).

## 1. Introduction

Humans have always had an intrinsic behavior to explore and investigate their surroundings, which led us to explore and conquer the Earth's land, sea, and sky. Save for only the deepest parts of the ocean, most of Earth has been explored, leaving space as the last frontier, with satellites currently as the main tool of exploration. However, it comes at a very expensive cost; a venture that was traditionally accessible to governments with huge discretionary funds only. With the introduction of miniaturization and commercialization of satellites, the democratization of space has begun and is now accessible to universities and small countries as well. Recently, there has been a renewed effort in space exploration. This is attributed to the introduction of a class of standardized miniature satellites called the CubeSat, and the commercialization of space technology. Its popularity can be attributed to the reduction in development and deployment costs and time, making space more accessible than in the past. As more microsatellites are used for space missions, the need for micro-propulsion systems increased, as many studies showed that the use of onboard propulsion systems can dramatically increase the capabilities, reliability, and lifetime by a factor of 2 to 3 [1].

Electric propulsion gradually became the optimal propulsion choice for microsatellites than chemical propulsion, as typical mission periods can be months or years. Chemical propulsion produces thrust based on chemical reactions of the propellant, which makes it dependent on the amount of propellant it carries. Additionally, the volatile propellant requires large space, size, and specialized storage, making it bulky and hard to implement

in microsatellites, such as a CubeSat, which need to strictly adhere to the standard size of a 10 cm cube and weigh less than 1 kg. Chemical thrusters are characterized by short burn time, large thrust, and low specific impulse, which is not ideal for long space missions as it will not complete it economically or within a reasonable timeframe [2–4].

Unlike chemical propulsion, electric propulsion uses techniques to convert electrical power to thrust. Electric propulsion is characterized by its small size, high reliability, high safety rating, low thrust, and high specific impulse [5]. As the usage and interest of microsatellites increased, many different types of electric propulsions were developed and are commercially available. However, they are extremely expensive, which is supported by large research grants offered to the best electric propulsion systems, and are normally proprietary research due to the commercial value it has [6].

Therefore, there is a current need for the development of a low-cost propulsion system solution for low-budgeted microsatellites, such as a Pocket-Cube, which is a 5 cm cube-shaped satellite weighing less than 250 g. It was developed and standardized as a satellite that could fit in a pocket; however, its low development cost makes it an attractive option for students and hobbyists with a low budget [7]. Its size, weight, and power are less than a CubeSat, which reduces costs and development time; however, this places more difficulty in the propulsion design, with no current commercial propulsion system available.

Pulsed plasma thrusters (PPTs) are a type of electric propulsion system that generate thrust by creating and accelerating a plasma discharge. PPTs have been extensively studied and developed for space propulsion applications due to their simplicity, reliability, and high specific impulse.

One study investigated the performance of a PPT using xenon propellant [8]. The study found that the thrust generated by the system was proportional to the square root of the applied voltage and the mass flow rate of the propellant.

Another study described the design and testing of a PPT for a CubeSat mission [3]. The study demonstrated the ability of the PPT to provide precise attitude control and station-keeping maneuvers for small spacecraft.

PPTs have also been used in various space missions, including the NASA Geotail mission [9] and the Japan Aerospace Exploration Agency's Hayabusa mission [10].

Overall, PPTs have shown promise as a propulsion technology for small spacecraft, and continued research and development in this field is likely to improve their performance and capabilities.

Additionally, it has a higher reliability than other types of propulsion due to its simplicity. Additionally, it is safer as it uses inert and non-toxic solid propellants, such as Teflon [2]. PPT can also operate on lower power levels than other propulsion system [1]. Thus, making it the ideal low-cost sub-joule propulsion solution for a Pocket-Cube.

## 2. Literature Review

PPT is categorized under electromagnetic propulsion [5]. It produces thrust by means of the Lorentz force ( $\vec{J} \times \vec{B}$ ), where the electromagnetic field created between two electrodes is used to accelerate highly ionized gas, called plasma, to create thrust [11]. It also uses some electrothermal propulsion to create thrust; however, the main propulsion of the PPT comes from electromagnetic propulsion [11].

A traditional PPT propulsion module contains a power source, a power processing unit (PPU), main-onboard computer (OBC), ignition (spark plug) unit, main energy bank, and the thruster, as seen in Figure 1 [11]. The PPU converts the satellite power supply to the required high voltage needed for the ignition unit's spark plug and the main energy bank [11]. The OBC functions as the control unit for the PPT's firing operation. The ignition unit contains the spark plug used to produce the pilot spark needed to initiate the main discharge, whereas the main energy bank is used to store the energy provided by the PPU. Capacitors are typically used as storage units for the PPU energy [11].

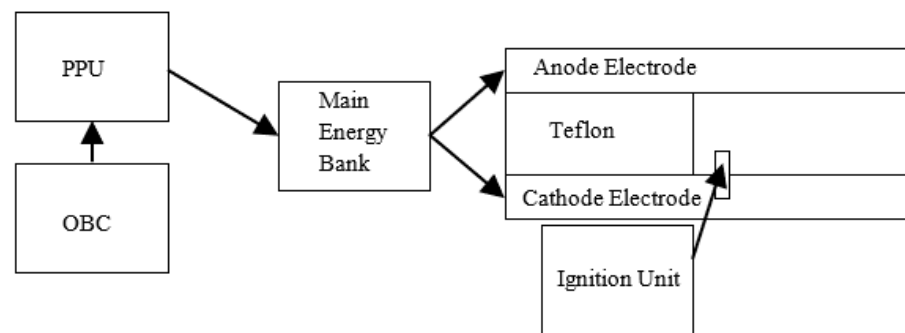


**Figure 1.** Basic PPT schematic.

A typical firing cycle for a traditional PPT starts after the main energy bank is charged. A pilot arc created from a spark plug produces electrons that impact the surface of the propellant with high velocity, as illustrated in Figure 2.

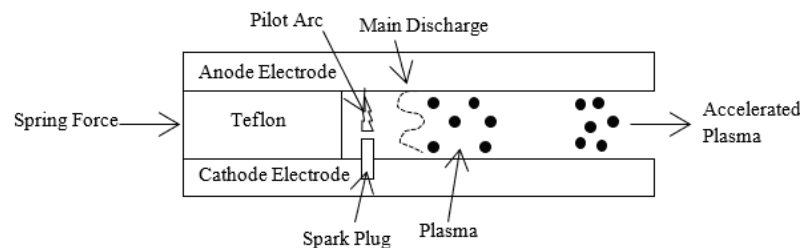


**Figure 2.** Operation of PPT.

The pilot arc creates small amounts of plasma. This is a neutral gas consisting of ions and electron particles, is electrically conductive, and can be manipulated by an electromagnetic field [2]. The initial pilot arc helps lower the impedance between the two electrodes, which initiates the main discharge from the energy bank between the two electrodes, resulting in ablation of the Teflon's surface. As a result, creates more plasma. The ablation process of Teflon creates more plasma, which is then ejected from the thruster due to the Lorentz force and the increased temperature and pressure [8].

### 2.1. PPT Configurations

PPT are classified according to the electrode configuration, and according to how the propellant is fed into the propulsion system, as seen in Table 1 [12].

**Table 1.** PPT configurations.

Electrodes Configuration	Propellant Configuration
Rectangular	Breach-Fed
Coaxial	Side-Fed

### 2.2. Rectangular Configuration

The most common configuration is the rectangular breach-fed configuration [13]. Two rectangular electrodes are placed parallel to each other, with Teflon placed between the two electrodes [11]. The current flow in the plasma from anode to the cathode interacts with the self-induced magnetic field, accelerating the plasma using the Lorentz Force [12], and flows downstream along the electrode's length [13]. Figure 3 shows a rectangular breach-fed configuration.

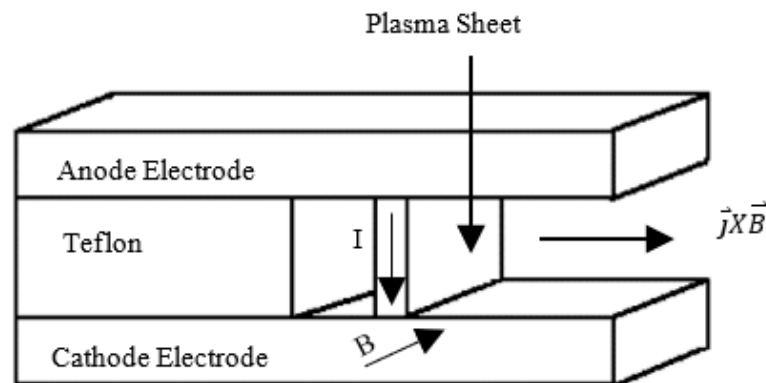


Figure 3. Rectangular PPT.

### 2.3. Coaxial Configuration

The electrodes are typically conical-shaped with a central (cathode) and outer electrode (anode), with Teflon between the two electrodes [12]. The ignitor is usually mounted in the cathode electrode [12,13]. By varying the diameter of the electrodes, the resistance can be controlled more easily than with a rectangular configuration [13]. Figure 4 shows a coaxial breech-fed configuration.

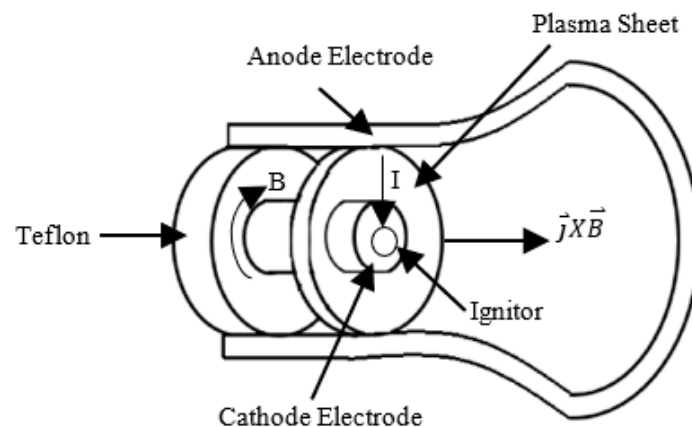


Figure 4. Coaxial PPT.

### 2.4. Breech-Fed and Side-Fed

Early prototypes of the PPT were the breech-fed propellant configuration with the side-fed configuration developed later [13]. The operation of the thruster depends on the propellant configuration in which the PPT can operate in ablation arc mode or propagation mode [13]. For breech-fed configuration, the force created by the main discharge propagates downstream away from the surface where the ablation occurs, thus having a reduced ablation surface, as illustrated Figures 3 and 4. However, a side-fed propellant configuration has the force parallel to the ablating surface, allowing it to maintain the ablation rate. The side-fed propellant configuration can be seen in Figure 5.

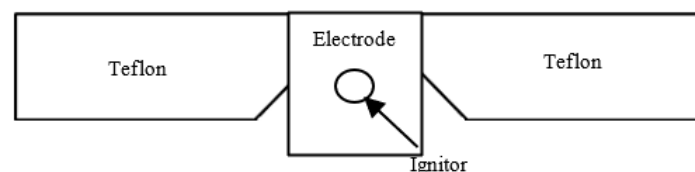


Figure 5. Rectangular Side-fed PPT.

A rectangular side-fed pulsed plasma thruster is a type of electric propulsion system that generates thrust by expelling ionized gas (plasma) out of a nozzle [14]. The basic

design consists of a rectangular chamber with a side-mounted cathode and an anode at the other end of the chamber.

When a high-voltage pulse is applied to the cathode, it emits electrons that ionize the gas inside the chamber, creating plasma. The plasma then flows towards the anode, generating a force that propels the spacecraft forward.

To improve efficiency, some designs include a magnetic field to confine the plasma and direct it towards the nozzle. The nozzle shape can also be optimized to increase the exhaust velocity and thrust.

Overall, a rectangular side-fed pulsed plasma thruster is a promising technology for small satellite propulsion, as it provides high specific impulse (i.e., efficient use of propellant) and low thrust, which is ideal for orbital maneuvers [15,16].

The literature lists several studies to find the optimal thruster characteristics; however, there are no standard formulas when it comes to designing and determining the performance of PPT. The list below summarizes previous studies completed on different thruster characteristics:

(1) Electrodes:

- Electrode Gap: Arrington et al. [17] found that increase in electrodes' space leads to a decrease in thrust-to-power ratio while specific impulse and efficiency increase. Mingo Pérez et al. [18] also found that excessive increase in electrode gap led to increase carbonization of Teflon.
- Electrode Width: Arrington et al. [17] found that increase in electrode width led to a decreased in thrust-to-power ratio while specific impulse and efficiency increases.
- Aspect ratio: The equation below shows the relationship between the thrust-to-power and aspect ratio. There is no limit to increasing the aspect ratio. For example, an aspect ratio as high as 30:1 was previously achieved [19]. However, a high aspect ratio resulted in a non-uniform electromagnetic field.

$$\frac{\text{Thrust}}{\text{Power}} \propto \frac{\text{Electrode width}}{\text{Electrode gap}}$$

The aspect ratio in pulsed plasma thrusters refers to the ratio of the length of the discharge channel to its diameter [20]. It is an important parameter that determines the efficiency and performance of the thruster. In general, a higher aspect ratio leads to a more efficient thruster because it allows for a longer ionization path, and therefore, more complete ionization of the propellant [21]. This leads to a higher thrust-to-power ratio and better overall performance. However, increasing the aspect ratio beyond a certain point can lead to increased instabilities in the discharge and reduced overall efficiency. Therefore, the optimal aspect ratio for a pulsed plasma thruster depends on a variety of factors, including the specific propellant being used, the desired thrust level, and the available power supply [21].

- Electrode Length: There have been contradicting studies in this area between Arrington et al. [17], and Guman and Peko [22]. Guman and Peko [22] concluded that a smaller electrode length produces more thrust-to-power at a specific impulse. However, Arrington et al. [17] concluded that increasing length increases the efficiency and specific impulse; however, no notable difference in thrust-to-power ratio was observed.
- Spark Plug Distance: Vondra et al. [23] found that the distance of the spark plug from the surface of the propellant influenced the performance of the PPT. The study showed that there is an optimum distance that can be reached in each PPT design, which was 1/16 inch (1.5 mm) to 3/16 inch (4.7 mm) for the study's PPT.

- Flare angle: The optimal flare angle between the electrode was found to be 20°, which resulted in an increase in thrust, impulse bits, thrust-to-power ratio, specific impulse, and increased the efficiency up to 35% [24].
  - Electrode shape: Tongue-shaped electrodes increased the specific impulse, impulse bits, and efficiency by almost 35% [24].
  - Segmented Electrodes: Studies conducted by Zhe et al. [25] found that electrodes that were segmented with a ceramic insulator resulted in an improved thrust efficiency of 49%, a higher current density of 75%, increase impulse bits of 28% and was also found to have better discharge topography.
- (2) Propellant [26–28]:
- Polymers Type: Experimental studies conducted by Scharlemann and York [27], and Palumbo and Guman [26] found that Teflon had the best performance overall when compared to other polymers.
  - Porosity: Pencil and Kamhawi [28] found that the porosity in Teflon increased the ablation rate, but it did not have any effect on the thrust produced.
  - Density: The higher the density of Teflon, the higher the electromagnetic component produced [28].
  - Carbon: Teflon, infused with carbon particles, had a slightly better specific impulse and efficiency than pure Teflon [28].
- (3) Spark Plug

The ignition system is one of the most critical parts of the thruster operation [13]. It consists of a spark plug and a high voltage circuit. The traditional spark plug consists of two electrodes to create an electric spark. It is important to the function of the thruster as it is needed to create the initial discharge to ablate the needed amount of Teflon in order to initiate the main discharge. However, ablation of Teflon creates a problematic by-product of carbon and fluorine, which can cause erosion and contamination of the ignitor electrode surface. This can severely reduce the ignitor's lifetime [29].

#### (4) Power System

The power system consists of a PPU (Power Processing Unit) and a capacitor bank for the ignitor and main discharge systems. It is responsible for supplying the required energy for the capacitor banks. The power available for the PPU is usually determined by considering the type of spacecraft. Available supply voltages can range from 3.3 V to 35 V. A flyback transformer, or a high voltage transformer is usually used to increase the voltage to several kV's for the capacitor banks and ignition system. There are many varieties of methods and PPU designs, with most power-to-weight ratio of 100 W/kg [11].

#### (5) Thrust Measurement

The performance of the PPT is measured in a vacuum on a thrust stand, which can be a pendulum or a deflecting beam, as shown in Figure 6 [13]. Thrust can be measured by measuring the impulse bits of each shot, multiplied by the pulse frequency operation of the thruster [5]. The minimal impulse bits produced by the thruster indicates the precision level of the thruster. Aheieva et al. [30] successfully used a micro-pendulum test stand to successfully measure impulse bit in the  $\mu\text{Ns}$  range [30]. Each displacement of the special mass of the pendulum was recorded with a high-speed camera. Equation (1) was used by Aheieva et al. [30] to calculate the impulse bits produced by the developed vacuum arc thrusters with known parameters of the micro-pendulum.

$$I_{bit} = F\Delta t = m_{pend} \sqrt{2g(L - \sqrt{L^2 - x^2})} \quad (1)$$



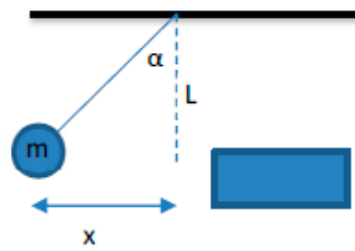


Figure 6. Micro-pendulum thrust stand.

### 3. Design Description

For the proposed PPT propulsion system with adjustable pulsed operation frequency and output voltage, we considered a combination of a circuit module and thruster module. The circuit module housed the PPU, main energy bank unit, ignition unit, and the control unit. One PPT module development costs were estimated to be less than 795 USD.

#### 3.1. Circuit Module Design Description

The proposed circuit module, described below, was designed to operate with an input voltage of 3.3 V or 5 V with a pulsed frequency range of 0.25 Hz~0.5 Hz. The circuit design costs was kept low by incorporating easily available Commercial-Off-the-Shelf (COTS) components costing \$32,341 USD, with the final designed PCB weighing less than 12 g. The following sub sections detail each of part of the circuit modules as illustrated in Figure 1.

##### 3.1.1. PPU

The PPU consisted of a Q20-5 ECMO (0.5 W) high voltage supply with isolated outputs that was powered from an Arduino UNO power bus (3.3/5 V). The Q20-5 is rated for an input voltage of 5 V; however, the manufacturer's datasheet states that it has a linearly dependent output. Therefore, for an input voltage of 3.3 V or 5 V, the output generated is 1.32 kV or 2 kV for the main energy bank and ignition circuit. An IC load connected to the Arduino UNO was used to switch the Q20-5 ECMO module on and off. The main energy bank unit consisted of two parallel ceramic capacitors with a total capacitance value of 0.136  $\mu$ F.

##### 3.1.2. Main Energy Bank Unit

Referring to Figure 7's green section. The main energy bank unit consisted of a 0.136  $\mu$ F ceramic capacitor, which is pulsed rated and recommended for capacitive discharge ignition (CDI) circuits. The capacitor bank was charged directly from the ECMO Q20-5 module. An amount of 1.32 kV or 2 kV from the ECMO Q20-5 gave the thruster an estimated energy of 0.118 J or 0.272 J per shot (depending on the input voltage used during the operation). The thruster's electrode was attached to the main bank capacitor as seen in Figure 7.

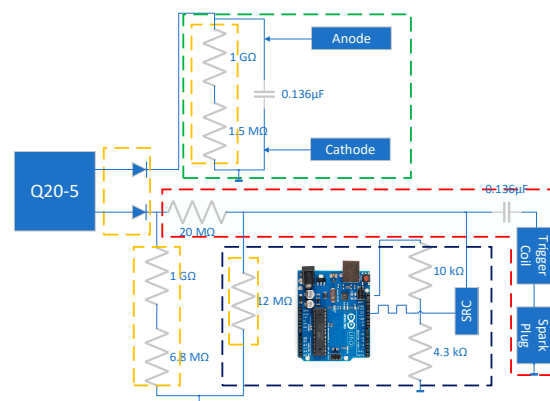


Figure 7. Circuit Schematic.

### 3.1.3. Ignition Unit

Referring to the red section in Figure 7, the high voltage from the ECMO Q20-5 module was reduced to 300 V and 750 V, depending on the input voltage, using 20 M $\Omega$  resistors. The reduced voltage was then stored in the ignition energy bank which consisted of a 0.1  $\mu$ F ceramic capacitor. The ignition capacitor bank was connected to an 800 V rated silicon-controlled rectifier (SCR) and trigger coil transformer. A trigger transformer was used to step up the voltage from the ignition capacitor bank with a winding ratio of 1:40. Therefore, with an input voltage of 3.3 V or 5 V, it had an output voltage of 12 kV or 30 kV.

### 3.1.4. Control Unit

Referring to the blue section of Figure 7, the control unit of the circuit module was used to control the firing of the thruster module at the desired frequency. This was done by sending a 5 V trigger pulse by the Arduino at the desired frequency (0.25 Hz/0.5 Hz). Thereafter, the 5 V trigger pulse was reduced to a 1 V trigger pulse, which was applied to the gate of the 800 V silicon-controlled rectifier (SRC). Once the 100 ms trigger pulse was applied to the gate of the SRC, the ignition capacitor discharged through the SRC, generating a huge current flow in the trigger coil, resulting in a high voltage output. The trigger coil was connected to the spark plug anode electrode plate. Figure 8 illustrates a detailed operation of the circuit during a single firing cycle of the thruster when the SRC is acting as an open or closed switch.

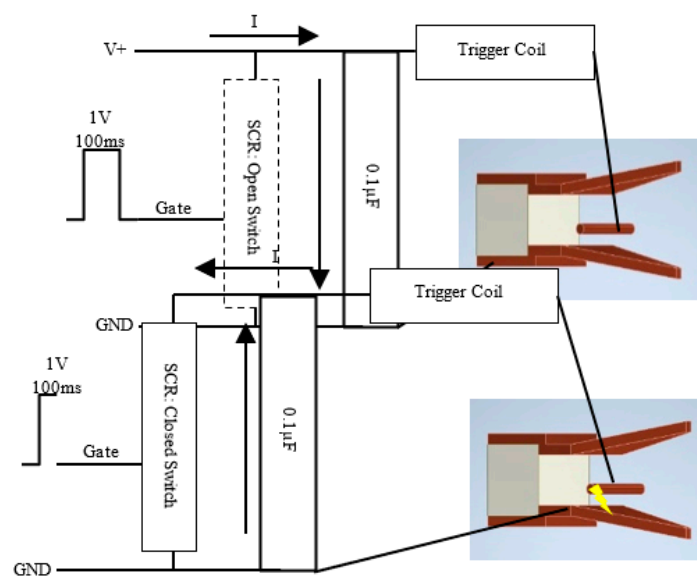


**Figure 8.** Firing Cycle of the Spark Plug.

### 3.1.5. Safety and Monitoring

Any excess energy left in the ignition capacitor bank was dissipated using a 12 M $\Omega$  resistor. Additionally, two high voltage dividers were added parallel to each capacitor bank, which was used to read the capacitor bank's voltage, for circuit fault finding and capacitor bank monitoring. Components, such as the Arduino UNO and ECMO high voltage supply, were protected by two 1.2 kV Schottky diodes. All safety and high voltage dividers components are illustrated in the orange section in Figure 7.

### 3.1.6. L-Shaped Notch PPT

In an L-shaped notch PPT, the plasma is generated by a high-voltage discharge in a small cavity with an L-shaped notch [31]. The L-shaped notch is designed to create a strong magnetic field that helps to confine the plasma and increase its density. The magnetic field is created by a current passing through a coil located near the notch.



When the discharge is initiated, the plasma is accelerated out of the cavity by the Lorentz force generated by the interaction between the plasma and the magnetic field. The plasma then expands into space, generating thrust [31].

The L-shaped notch design has several advantages over other PPT designs. For example, it allows for a higher plasma density and better confinement, which increases the efficiency of the thruster. Additionally, the L-shaped notch PPT is relatively simple to construct and operate, making it a popular choice for small spacecraft and CubeSats [31].

However, one disadvantage of the L-shaped notch PPT is that it tends to produce a large amount of electromagnetic interference (EMI) due to the high current passing through the coil. This can be a concern for sensitive electronics on board the spacecraft, and measures may need to be taken to mitigate the EMI.

### 3.2. Thruster Module Design Description

The PPT propulsion system was developed by means of the iterative design method, in which the designs were reviewed and improved upon until the final design satisfied all the design requirements. It focused on simplifying and improving on the traditional PPT design, as discussed in the previous literature review section, with minimal machining.

The thruster module was based on a traditional breech-fed rectangular PPT configuration. The thruster module consisted of the Teflon propellant block, spring-fed propellant system consisting of a spring, copper electrodes, 3D printed ULTEM 1010 thermoplastic housing, and copper spark plug wire, as shown in Figure 9. The two electrodes and the housing both have an L-shaped notch integrated into their design, which, when mated, uses the spring force from the spring-fed propellant system to keep the electrodes and the propellant block in position, as shown in Figure 10. The propellant used was a 10 mm Teflon cube weighing 2 g, and the anode and cathode electrodes were 1.5 mm thick with an aspect ratio of 1 and 20 mm length. The electrodes were also designed to be tongue-shaped with a 20° flare angle as reviewed in the literature section and shown in Figure 3.

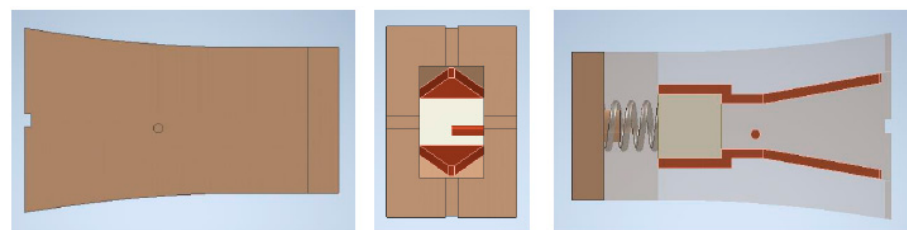


Figure 9. Final CAD of PPT.

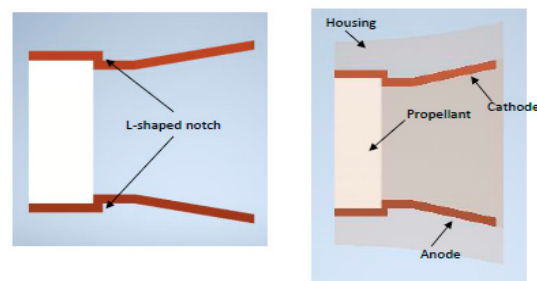


Figure 10. L-shaped Notch.

Available commercial spark plugs such as the Rimfire Micro Viper Z3 spark plug are expensive (\$35), bulky, and require their own PPU and control unit, which makes it unsuitable for a Pocket-Cube. A breakdown of the spark plug shows that a spark plug fundamentally consists of two electrodes, an anode, and a cathode, placed at a close distance to create a spark via a high voltage breakdown. Therefore, the spark plug unit was able to be reduced to a 1.5 mm diameter copper wire used as the anode, which was placed 3 mm

away from the cathode electrode plate of the thruster and 3 mm away from the propellant surface. The spark plug can be seen in Figures 4 and 5.

As seen in Figure 11, the spark plug unit was simplified with a copper wire using the cathode electrode plate as the ground, which reduced the size and weight of the thruster to  $10 \times 1.5 \times 1.5$  mm, compared to a commercial spark plug, such as the Rimfire Micro Viper Z3, which is  $18.54 \times 5.84 \times 5.84$  mm. However, the extreme simplification of the spark plug design resulted in a reduced lifetime. The thruster was chosen to be printed in ULTEM, which is a thermoplastic filament with properties, such as a high melting point ( $200^\circ\text{C}$ ), and good heat and electric insulator properties. The 3D printed ULTEM thruster unit with Teflon brought the total thruster unit weight to 32 g, with a total size of  $50 \times 29 \times 20$  mm, and a cost of less than \$132 USD. Figure 9 shows the CAD of the final thruster unit and a summary of the iterative design method is indicated in Figure 12.

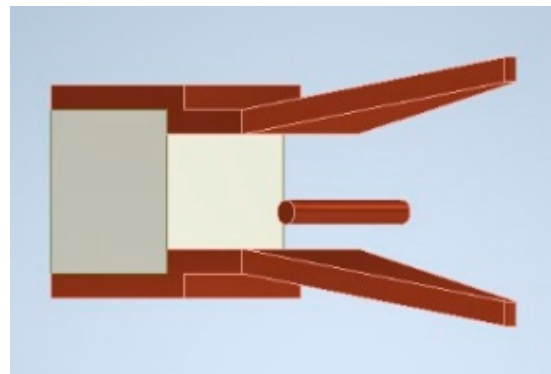


Figure 11. CAD of Spark Plug with the electrodes.

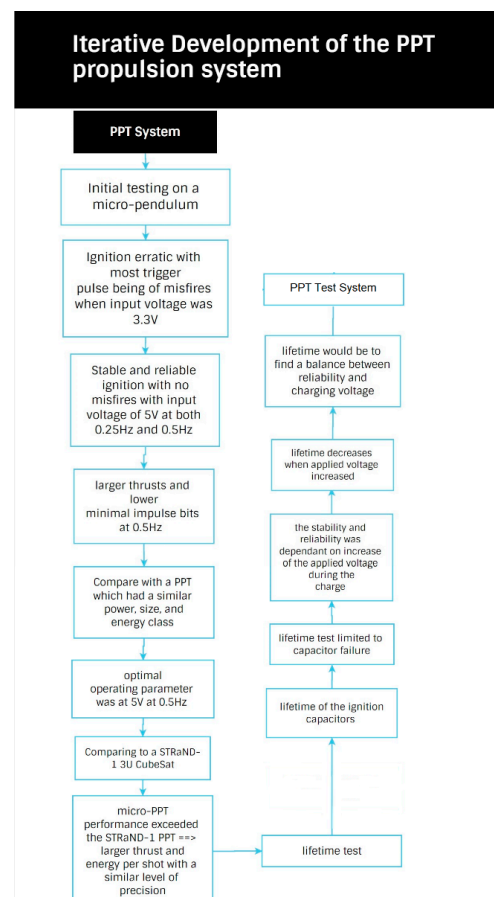
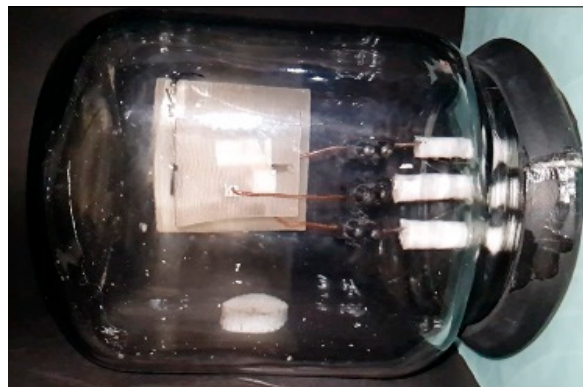


Figure 12. Summary of the iterative design process.

#### 4. Experimental Setup

The thruster was tested in a glass vacuum chamber under a pressure reading of  $-720$  mmHg ( $-96$  kPa). Performance data of the developed thruster was collected using a 3D printed micro-pendulum test stand, as seen in Figure 13, and recorded using the slow-motion video mode of a Samsung S8 camera. Aheieva et al. [30] successfully used a micro-pendulum test stand to successfully measure impulse bit in the  $\mu\text{Ns}$  range [30], as explained in Section 2.4 number 5 (Thrust measurement) and Figure 6. The micro pendulum test stand has a special target mass, made from SCS 1000 plastic film with an estimated weight of  $0.0182$  g, and attached to a very thin copper wire length of  $40$  mm. A program called Tracker was used to measure the inclination angle recorded for each shot. Equation (1) in the literature section was used to calculate the impulse bits and thrust produced during the testing [30].



**Figure 13.** Micro-pendulum Test Stand inside the vacuum chamber.

#### 5. Experimental Results

##### 5.1. Performance Test

The circuit unit was tested for ignition reliability under atmospheric conditions, which was achieved at a pulsed ignition spark at both  $3.3$  V and  $5$  V at a frequency of  $0.25$  Hz, respectively, with no electric arc between the components.

Thereafter, once the desired vacuum pressure was achieved, the thruster was tested for performance at two input voltages of  $3.3$  V and  $5$  V. It was first tested with the input voltage of  $3.3$  V at  $0.5$  Hz. During the first  $50$  shots, the thruster was unsuccessful as it had erratic ignition with repetitive misfires; therefore, testing was terminated. The frequency was lowered to  $0.25$  Hz at the same input voltage of  $3.3$  V; however, the thruster still had performance issues of erratic ignition with many repetitive misfires. Using the high voltage divider design into the circuit, the main capacitor bank measured a voltage of  $940$  V, which showed that the EMCO Q20-5 module output was not linearly dependent as stated in the datasheet. Therefore, lower voltages produced by the ECMO Q20-5 caused the erratic ignition, and misfires were due to a lower applied voltage of  $940$  V, which caused lower energy in the ignition and main energy bank.

Next, the PPT was tested at an input voltage of  $5$  V, which was able to achieve reliable and stable firing operation of the PPT propulsion system at both frequencies of  $0.25$  Hz and  $0.5$  Hz. At each frequency,  $120$  shots were recorded and analyzed. The results showed that at  $0.25$  Hz, the micro-PPT produced an inclination angle range of  $4.2$  degrees to  $14.3$  degrees, which calculated to a minimum impulse bit (MIB) of  $0.838$   $\mu\text{N}$ , with an average thrust of  $0.387$   $\mu\text{N}$ . For operation at  $0.5$  Hz, the micro-PPT was able to produce an inclination angle range of  $3.5$  degrees to  $10.6$  degrees, which calculated to a minimum impulse bit of  $0.698$   $\mu\text{Ns}$ , with an average thrust of  $0.713$   $\mu\text{N}$ . It showed that the thruster operated best at  $0.5$  Hz, as it resulted in the lowest minimum impulse bits and produced the larger average thrust. The enhanced performance of the micro-PPT could be attributed to the operating frequency of  $0.5$  Hz contributing to higher temperature, which improved the electrothermal

operation of the micro-PPT and creation of plasma, thus making the thruster more efficient and precise. The testing also showed that the thruster ignition stability depends heavily on the voltage applied to the main and ignition capacitor bank.

Performance results of the PPT at 0.5 Hz with the input voltage of 5 V was compared to a PPT designed and developed for the STRaND-1 3U CubeSat. The results showed that despite operating at one third of the power of the STRaND-1, the PPT has a similar minimum impulse bit, a larger energy per shot, larger average thrust, and faster operating frequency. This shows that the developed micro-PPT's design was successfully optimized through the iteration design process of simplification and improvements made to the traditional PPT design, making it a very attractive propulsion option for the Pocket-Cube due to the low manufacture costs and simplicity. Table 2 shows a summary of the comparison [11].

**Table 2.** Comparison of PPT and STRaND-1 PPT.

Thruster	V <sub>in</sub> (V)	Power (W)	Time (s)	Energy (J)	Min. Impulse Bit (μNs)	Ave. Thrust (μN)
STRaND-1	5	1.5	6	0.19	0.56	0.09
Micro-PPT	5	0.5	2	0.272	0.698	0.713

### 5.2. Plasma Plume

During the test and video analysis, it was observed that the thruster produced visible plasma plumes only at certain shots, with most seen in the operating frequency of 0.5 Hz. This is due to the micro-PPT not ablating enough Teflon, which results in lower plasma plume density. Hence, less visibility of the plasma plume. However, whether the plasma plume was visible or not on the video, it did not result in a huge difference of inclination angle produced by the micro-PPT. Therefore, the developed thruster's performance did not heavily depend on the ablation of Teflon to operate. It was also noted during video analysis that there was a clear time delay of 0.01 s (1 frame) between the firing and plasma evolution to the interaction of the micro-pendulum.

### 5.3. Lifetime Test

A quantifiable lifetime test was conducted of the propulsion system in a vacuum environment. The PPT was operated at the optimal parameters of pulsed frequency of 0.5 Hz with an input voltage of 5 V, until pulsed operation ceased. During the first lifetime test, the PPT operated for 18 min (540 shots) with continuous and reliable ignition, that is, no misfires were detected, until it failed due to the main bank's capacitor failure. The capacitor failure was attributed to it being overdriven with a higher voltage of 2 kV over a longer period than the datasheet recommended. Even if the capacitor is rated at 2 kV, the nominal rated voltage is 1 kV. The second lifetime test was conducted with a new capacitor at a reduced input voltage of 4 V, instead of the maximum 5 V. This was done to reduce the burden on the main capacitor bank. The thruster operated with the main energy bank voltage of 1.6 kV, in which the thruster produced 0.174 J per shot. However, after a 40 min period (~1200 shots), the operation ceased again due to capacitor failure. The total shots fired from the thruster was 1740 shots during the lifetime test, with a total of 1980 shots fired during the whole test. This is very low compared to the PPT developed by Clark et al. [32] for a CubeSat, which had a lifetime of 1,500,000 shots. The lifetime test showed that the propulsion system lifetime was influenced by the charging voltage applied to the capacitor and depended heavily on the capacitor's lifetime. However, as shown in the previous tests, the ignition reliability and stability increased as the applied voltage increased. Therefore, a balance between the two is critical to the PPT lifetime and stable operation.

#### 5.4. Physical Inspection

A physical inspection of the thruster unit did not show signs of significant erosion or charring of the electrodes, spark plug, or notable reduction in propellant weight. Upon a closer inspection, some char spots can be seen with a slight char and erosion at the spark plug and electrodes, as shown in Figures 14 and 15. The surface of the Teflon is also slightly rough with a few shallow lines where ablation of the Teflon occurred, as shown in Figure 16.



Figure 14. Before and after on cathode electrode.



Figure 15. Erosion and char on spark plug anode electrode.



Figure 16. Before and after on propellant cube.

#### 6. Conclusions

The first generation of low-cost sub-joule micro-PPT propulsion system for a Pocket-Qube was successfully designed, developed, and tested using typical equipment available to students and hobbyists with minimal machining. This was achieved through the iterative design process that focused on simplification and improvement upon the traditional PPT design. The developed micro-PPT was able to achieve a large reduction in the costs, power, weight, and size, and meet all the design requirements as set out.

Initial testing of the micro-PPT on a micro-pendulum established that the optimal operating parameter for the micro-PPT propulsion system was 5 V at 0.5 Hz. It was discovered during tests that the micro-PPT's ignition was erratic with most trigger pulses being misfires when the input voltage was 3.3 V, due to the lower voltage output than expected. The micro-PPT was able to achieve stable and reliable ignition with no misfires with an input voltage of 5 V at both 0.25 Hz and 0.5 Hz, respectively. This showed that the voltage applied to the ignition and main capacitor bank directly influenced the reliability and stability of the micro-PPT operation. Additionally, there was a larger thrusts and lower minimal impulse bits at 0.5 Hz, to which the improved performance was attributed to the improved electrothermal efficiency of the micro-PPT through observation of the plasma plume.

Afterwards, a comparison was made with a PPT, which had a similar power, size, and energy class. It showed that the micro-PPT's impulse bits and thrusts were found to be within a reasonable range. Compared to a STRaND-1 3U CubeSat, the micro-PPT performance exceeded the STRaND-1 PPT as it produced with a larger thrust and energy per shot with a similar level of precision. However, the reduction in the costs, size, power, weight, and simplification of the design and manufacturing makes it a more compelling propulsion system option for a Pocket-Qube than the STRaND-1's PPT.

After the lifetime test, the micro-PPT was able to fire 1980 shots with no visible indication of significant wear, charring, or erosion of the electrodes and spark plug, and no significant propellant depletion. However, the key factor limiting the lifetime of the



micro-PPT propulsion system was the limiting lifetime of the ignition capacitors. Every lifetime test conducted was terminated due to capacitor failure, which was attributed to the capacitors being overdriven. This was evident when the voltage was dropped from 5 V to 4 V at 0.5 Hz, resulting in a lifetime increase from 540 shots to 1200 shots.

The charging voltage applied during the charging period greatly influenced the lifetime of the capacitor. However, as shown in previous tests, the stability and reliability of the micro-PPT ignition was dependent on the increase in the applied voltage during the charge, while the lifetime decreases when the applied voltage increased. Therefore, the solution for extending the lifetime would be to find a balance between reliability and lifetime for the micro-PPT.

Future recommendations on micro-PPT would be to replace and find more highly reliable pulse capacitors with a higher rated voltage for a more extended lifetime. This will ensure that the micro-PPT would be able to have enough tolerance without it being overdriven, while maintaining the desired high voltage and energy for successful and reliable ignition of the micro-PPT. Additionally, another capacitor bank can be added to share the load, therefore improving the lifetime of the load, although at the cost of increase cost, size, and weight. To further increase ignition reliability, additional improvements can be made to the spark plug to increase the voltage breakdown, reliability, and lifetime through improvements to the ignitor profile design, manufacturing process, and new ignitor materials.

**Author Contributions:** Conceptualization, J.B. and F.S.; methodology, J.B.; software, J.B.; validation, J.B.; formal analysis, J.B. and F.S.; investigation, J.B.; resources, F.S.; data curation, J.B.; writing—original draft preparation, J.B. and F.S.; writing—review and editing, F.S.; visualization, J.B. and F.S.; supervision, F.S.; project administration, F.S.; funding acquisition, F.S. All authors have read and agreed to the published version of the manuscript.

**Funding:** This research received no external funding.

**Institutional Review Board Statement:** Not applicable.

**Informed Consent Statement:** Not applicable.

**Data Availability Statement:** Data is contained within the article or supplementary material. The data presented in this study are available in [http://vital.seals.ac.za:8080/vital/access/manager/Repository/vital:58953?site\\_name=GlobalView](http://vital.seals.ac.za:8080/vital/access/manager/Repository/vital:58953?site_name=GlobalView).

**Conflicts of Interest:** On behalf of all authors, the corresponding author states that there is no conflict of interest.

## References

1. Pottinger, S.; Scharlemann, C. Micro Pulsed Plasma Thruster Development. In Proceedings of the 30th International Electric Propulsion Conference, Florence, Italy, 17–20 September 2007.
2. Johnson, I.K. The Development of a Pulsed Plasma Thruster as a Solid Fuel Plasma Source for a High Power Helicon. Master's Thesis, The University of Washington, Seattle, WA, USA, 2011.
3. Ciaralli, S.; Coletti, M.; Gabriel, S. Performance and lifetime testing of a pulsed plasma thruster for Cubesat applications. *Aerosp. Sci. Technol.* **2015**, *47*, 291–298. [\[CrossRef\]](#)
4. Ciaralli, S.; Coletti, M.; Gabriel, S. Results of the qualification test campaign of a Pulsed Plasma Thruster for Cubesat Propulsion (PPTCUP). *Acta Astronaut.* **2016**, *121*, 314–322. [\[CrossRef\]](#)
5. Burton, R. *Encyclopedia of Aerospace Engineering*; John Wiley & Sons, Ltd.: Hoboken, NJ, USA, 2010.
6. Manzella, D. *Low Cost Electric Propulsion Thruster for Deep Space Robotic Missions*; NASA: Washington, DC, USA, 2007.
7. Moon, M. PocketQube Kits Make It Easier for Amateurs to Build Their Own Satellites. Engadget. Available online: <https://www.engadget.com/2014-12-17-pocketqube-kits.html> (accessed on 6 February 2022).
8. Ketsdever, A.D.; Lee, R.H.; Lilly, T.C. Performance testing of a microfabricated propulsion system for nanosatellite applications. *J. Micromech. Microeng.* **2005**, *15*, 2254. [\[CrossRef\]](#)
9. Nishida, A.; Uesugi, K.; Nakatani, I.; Mukai, T.; Fairfield, D.; Acuna, M. Geotail mission to explore earth's magnetotail. *Eos Trans. Am. Geophys. Union* **1992**, *73*, 425–429. [\[CrossRef\]](#)
10. Kawaguchi, J.I. The Hayabusa mission—Its seven years flight. In *2011 Symposium on VLSI Circuits—Digest of Technical Papers*; IEEE: Piscataway, NJ, USA, 2011; pp. 2–5.



11. Shaw, P. Pulsed Plasma Thrusters for Small Satellites. Ph.D. Thesis, University of Surrey, Guildford, UK, 2011.
12. Patel, A. Magnetically Levitating Low-Friction Test Stand for the Evaluation of Micro-Thrusters. Master's Thesis, The University of Alabama, Tuscaloosa, Alabama, 2015.
13. Burton, R.L.; Turchi, P.J. Pulsed Plasma Thruster. *J. Propuls. Power* **1998**, *14*, 716–735. [[CrossRef](#)]
14. Rosales, M.A. *Investigation of a Pulsed Plasma Thruster for Atmospheric Applications*; University of Washington: Seattle, WA, USA, 2020.
15. Wu, Z.; Huang, T.; Liu, X.; Lin, W.Y.L.; Wang, N.; Ji, L. Application and development of the pulsed plasma thruster. *Plasma Sci. Technol.* **2020**, *22*, 094014. [[CrossRef](#)]
16. Gessini, P.; Possa, G.C.; Marques, R.I.; Dobranszki, C.; Golosnoy, I.O.; Gabriel, S. Enabling low-cost high-energy missions with small spacecraft by using pulsed plasma thrusters. In Proceedings of the 36th International Electric Propulsion Conference: IEPC, Vienna, Austria, 15–20 September 2019.
17. Arrington, L.; Haag, T.; Pencil, E.; Meckel, N. *A Performance Comparison of Pulsed Plasma Thruster Electrode Configurations*; NASA: Washington, DC, USA, 1998.
18. Pérez, A.M.; Coletti, M.; Gabriel, S.B. Development of a Microthruster Module for Nanosatellite Applications. In Proceedings of the 32nd International Electric Propulsion Conference, Wiesbaden, Germany, 11–15 September 2011.
19. Ketsdever, A.D.; Micci, M.M. (Eds.) . *Micropropulsion for Small Spacecraft*; AIAA: San Diego, CA, USA, 2000; Volume 187.
20. Pottinger, S.J.; Krejci, D.; Scharlemann, C.A. Pulsed plasma thruster performance for miniaturised electrode configurations and low energy operation. *Acta Astronaut.* **2011**, *68*, 1996–2004. [[CrossRef](#)]
21. Mazouffre, S. Electric propulsion for satellites and spacecraft: Established technologies and novel approaches. *Plasma Sources Sci. Technol.* **2016**, *25*, 033002. [[CrossRef](#)]
22. Guman, W.; Peko, P. Solid-propellant pulsed plasma microthruster studies. *J. Spacecr. Rocket.-J. Spacecr. Rocket* **1968**, *5*, 732–733. [[CrossRef](#)]
23. Vondra, R.; Thomasse, K.; Solbes, A. Analysis of Solid Teflon Pulsed Plasma Thruster. *J. Spacecr.* **1970**, *7*, 1402–1406. [[CrossRef](#)]
24. Schönherr, T.; Nawaz, A.; Herdrich, G.; Röser, H.-P.; Auweter-Kurtz, M. Influence of Electrode Shape on Performance of Pulsed Magnetoplasmdynamic Thruster SIMP-LEX. *J. Propuls. Power* **2009**, *25*, 380–386. [[CrossRef](#)]
25. Zhe, Z.; Ren, J.; Tang, H.-B.; Ling, W.; York, T. An ablative pulsed plasma thruster with a segmented anode. *Plasma Sources Sci. Technol.* **2017**, *27*, 015004. [[CrossRef](#)]
26. Palumbo, D.; Guman, W. Effects of Propellant and Electrode Geometry on Pulsed Ablative Plasma Thruster Performance. *J. Spacecr. Rocket.* **1976**, *13*, 163. [[CrossRef](#)]
27. Scharlemann, C.; York, T. Alternative Propellants for Pulsed Plasma Thruster. In Proceedings of the 38th AIAA/ASME/SAE/ASEE Joint Propulsion Conference & Exhibit, Indianapolis, Indiana, 7–10 July 2002.
28. Pencil, E.; Kamhawi, H. Alternate Propellants Evaluation for 100-Joule-Class Pulsed Plasma Thrusters. In Proceedings of the 39th AIAA/ASME/SAE/ASEE Joint Propulsion Conference and Exhibit, Huntsville, AL, USA, 20–23 July 2003.
29. Wu, J.; Zhang, Y.; Cheng, Y.; Huang, Q.; Li, J.; Zhu, X. Plasma Generation and Application in a Laser Ablation Pulsed Plasma Thruster. In *Plasma Science and Technology-Basic Fundamentals and Modern Applications*; IntechOpen: London, UK, 2018.
30. Aheieva, K.; Toyoda, K.; Cho, M. Vacuum Arc Thruster Development and Testing for Micro and Nano Satellites. *Trans. Jpn. Soc. Aeronaut. Space Sci. Aerosp. Technol. Jpn.* **2016**, *14*, Pb\_91–Pb\_97. [[CrossRef](#)] [[PubMed](#)]
31. Scougal, E.A.; Marchetto, J.D.; Eslava, S.A. *Design of a Micro-Pulsed Plasma Thruster for a 3U Cubesat*; Worcester Polytechnic Institute: Worcester, MA, USA, 2014.
32. Clark, C.; Guarducci, F.; Coletti, M.; Gabriel, S.M. An Off-the-Shelf Electric Propulsion System for CubeSats. 2011. Available online: <https://digitalcommons.usu.edu/smallsat/2011/all2011/46/> (accessed on 11 April 2020).

**Disclaimer/Publisher's Note:** The statements, opinions and data contained in all publications are solely those of the individual author(s) and contributor(s) and not of MDPI and/or the editor(s). MDPI and/or the editor(s) disclaim responsibility for any injury to people or property resulting from any ideas, methods, instructions or products referred to in the content.